CORTEX 117 (2019) 157–167

Available online at www.sciencedirect.com

ScienceDirect

Journal homepage: www.elsevier.com/locate/cortex

Research Report

Action at a distance on object-related ventral temporal representations

Dongha Lee[a,b], Bradford Z. Mahon [c,d,e,f] and Jorge Almeida[a,b,*]

[a] Proaction Laboratory, Faculty of Psychology and Education Sciences, University of Coimbra, Portugal
[b] Faculty of Psychology and Education Sciences, University of Coimbra, Portugal
[c] Department of Psychology, Carnegie Mellon University, Pittsburgh, PA, USA
[d] Center for Visual Science, University of Rochester, Rochester, NY, USA
[e] Department of Neurosurgery, University of Rochester, Rochester, NY, USA
[f] Department of Neurology, University of Rochester, Rochester, NY, USA

ARTICLE INFO

Article history:
Received 13 September 2018
Reviewed 15 November 2018
Revised 7 January 2019
Accepted 23 February 2019
Action editor Stephen Jackson
Published online 4 March 2019

Keywords:
Local processing
Long-range connectivity
fMRI
tDCS
Tools

ABSTRACT

The representation of objects in ventral temporal cortex is relatively resilient to transformations in the stimuli. There is emerging recognition that ventral temporal object representations are forged via interactions among a broader network of regions that receive independent inputs about a stimulus. Here we test whether ventral temporal representations are causally modulated by disrupting processing in distal associative areas. We used transcranial direct current stimulation (tDCS) to stimulate left parietal areas and functional Magnetic Resonance Imaging (fMRI) to measure object-related neural responses in the ventral stream. We find that representational geometries and category discriminability within ventral temporal cortex, as well as functional connectivity between ventral temporal and parietal areas, are enhanced by anodal compared to cathodal stimulation of left parietal associative cortex. These results demonstrate that ventral temporal representations can be causally modulated by processing distal to the ventral stream.

Object representations in high-level associative visual cortex should ultimately be invariant to identity-preserving transformations in the way objects present themselves (e.g., DiCarlo, Zoccolan, & Rust, 2012). This is dictated by the fact that humans can (and have to) identify objects irrespective of the fact that every encounter with them will most times lead to different activation patterns within low-level visual areas. Several studies have demonstrated that neural responses within ventral temporal cortex – typically regarded as the *locus* of object recognition (e.g., Goodale & Milner, 1992; Orban, 2008; Rolls, 2000) – are indeed stable across the presentation of different exemplars of the same basic level object (e.g.,

* *Corresponding author*. Faculty of Psychology and Education Sciences, University of Coimbra, Rua do Colégio Novo, 3001-802 Coimbra, Portugal.
E-mail address: jorgealmeida@fpce.uc.pt (J. Almeida).
https://doi.org/10.1016/j.cortex.2019.02.018
0010-9452/

Quiroga, Reddy, Kreiman, Koch, & Fried, 2005) or different views of the same stimulus (e.g., Grill-Spector et al., 1999; James, Humphrey, Gati, Menon, & Goodale, 2002; Vuilleumier, Henson, Driver, & Dolan, 2002). This representational invariance allows for the necessary generalization power for optimal object recognition.

High-level object representations are, however, forged from the integration of information across distributed processing modules, and hence must be malleable enough to input from other higher-level cortical areas (e.g., Price & Devlin, 2011). In fact, cognitive processing and global brain functioning seem to follow strategies that are typical of small-world networks – local segregation in modules that are dedicated to particular aspects of information, and global integration of information within a network (although in this case connectivity can be long-distance; e.g., Deco, Jirsa, & McIntosh, 2011; Deco, Tononi, Boly, & Kringelbach, 2015; Park & Friston, 2013; see Fig. 1A). Specifically, local segregation seems to be implemented within ventral temporal cortex (and perhaps other locations in the brain) via a mosaic of regions that seem to prefer stimuli from one category over stimuli from other categories (e.g., Almeida, Fintzi, & Mahon, 2013; Chao, Haxby, & Martin, 1999; Downing, Jiang, Shuman, & Kanwisher, 2001; Epstein & Kanwisher, 1998; Garcea, Kristensen, Almeida, & Mahon, 2016; Kanwisher, McDermott, & Chun, 1997; Kristensen, Garcea, Mahon, & Almeida, 2016; Mahon, Kumar, & Almeida, 2013; Noppeney, Price, Penny, & Friston, 2006; for a review see Grill-Spector & Malach, 2004). Global integration of information processed within these segregated modules seems to be accomplished through long-range connections (e.g., Deco et al., 2015; Park & Friston, 2013), according to specific connectivity constrains, and flexibly integrating different types of information from different modules depending on the task at hand (e.g., Chen, Garcea, Almeida, & Mahon, 2017; Mahon, 2015; Op de Beeck, Haushofer, & Kanwisher, 2008). But how does a network integrate information across its modules? One intriguing possibility is for individual modules to convey information through long-range connections to other modules of the network (e.g., Almeida et al., 2013; Chen, Garcea, & Mahon, 2016; Mahon et al., 2007; Mahon et al., 2013), thus causally modulating information integration and representation distally within the network. That is, information processing within a module of a network may causally impact how information is represented in a distal module of that same network.

Here we test for this hypothesis by focusing on 3 categories – those of tools, faces and places/scenes – and exploiting some of the characteristic features of the architecture of the associated category-preferring networks; and by using neuromodulation (and specifically transcranial direct current stimulation – tDCS) to address how information is integrated and represented within a network. We used the tool-preferring network as our target network because it includes modules that are widespread, affording a series of long-range connections along with local segregation, and because some of the modules are readily accessible to neuromodulation techniques. This network includes the left inferior parietal lobule (IPL), bilateral superior and posterior parietal cortex, left posterior middle temporal gyrus (MTG), and bilateral (but stronger on the left) medial fusiform gyrus (mFUG; e.g., Almeida et al., 2013; Chao & Martin, 2000; Garcea & Mahon, 2014; Mahon et al., 2007, 2013; Noppeney et al., 2006). Importantly, these modules are functionally and anatomically connected with one another (Almeida et al., 2013; Chen et al., 2017; Garcea & Mahon, 2014; Hutchison, Culham, Everling, Flanagan, & Gallivan, 2014; Hutchison & Gallivan, 2016; Kravitz, Saleem, Baker, & Mishkin, 2011; Kravitz, Saleem, Baker, & Ungerleider, 2013; Mahon et al., 2013; Noppeney et al., 2006; Rushworth, Behrens, & Johansen-Berg, 2006; Simmons & Martin, 2012; Stevens, Tessler, Peng, & Martin, 2015) – specifically, strong connections have been observed between the left IPL and the left mFUG (e.g., Almeida et al., 2013; Garcea & Mahon, 2014; Hutchison et al., 2014; Mahon et al., 2013). Thus, by modulating activity at one of the modules of this network – e.g., the left IPL – we are able to probe a distal module of the network – e.g., the left mFUG – for effects at the level of multivariate information integration and representation.

Moreover, we can also test for the level of specificity at which the modulation of information processing takes place by 1) inspecting category-preferring regions that neighbor the left mFUG but present different category preferences, such as the left fusiform face area (FFA) that putatively prefers images of faces to images of stimuli from other categories (e.g., Kanwisher et al., 1997, but see Gauthier, Tarr, & Anderson, 1999; see Fig. 1C); and by 2) exploiting the fact that the left mFUG also shows a preference for places/scenes when compared to other categories such as animals or faces (Chen et al., 2016; Mahon et al., 2007). The strong hypothesis under test here is then that modulating neural responses within the left IPL – a module of the tool-preferring network – should lead to observable effects at the level of information integration and representation (as assessed by representation similarity and pattern discriminability) that are specific for modules within the tool-preferring network – i.e., effects should be visible only at the left mFUG, and not at the neighboring left FFA – and that are specific for the preferred category of the stimulated node – i.e., effects should be present for tool stimuli, but not for face or place stimuli.

Importantly, we use tDCS as our stimulation technique (Almeida et al., 2017; Batsikadze, Moliadze, Paulus, Kuo, & Nitsche, 2013; López-Alonso, Cheeran, Río-Rodríguez, & Fernández-del-Olmo, 2014; Stagg & Nitsche, 2011). tDCS is a non-invasive neuromodulation technique that modulates neural activity likely by interfering with resting membrane potential and synaptic strength via long-term potentiation or depression (e.g., Stagg & Nitsche, 2011). In fact, tDCS effects are typically considered activity-dependent (e.g., Fertonani & Miniussi, 2016; Fregni et al., 2005; Gill, Shah-Basak, & Hamilton, 2015; Senço, Huang, D'Urso, Parra, Bikson et al., 2015; Stagg & Nitsche, 2011). This certainly makes tDCS highly appropriate for studying (and intervening on; e.g., Martins, Fregni, Simis, & Almeida, 2017) domain-specific processes of the kind investigated here.

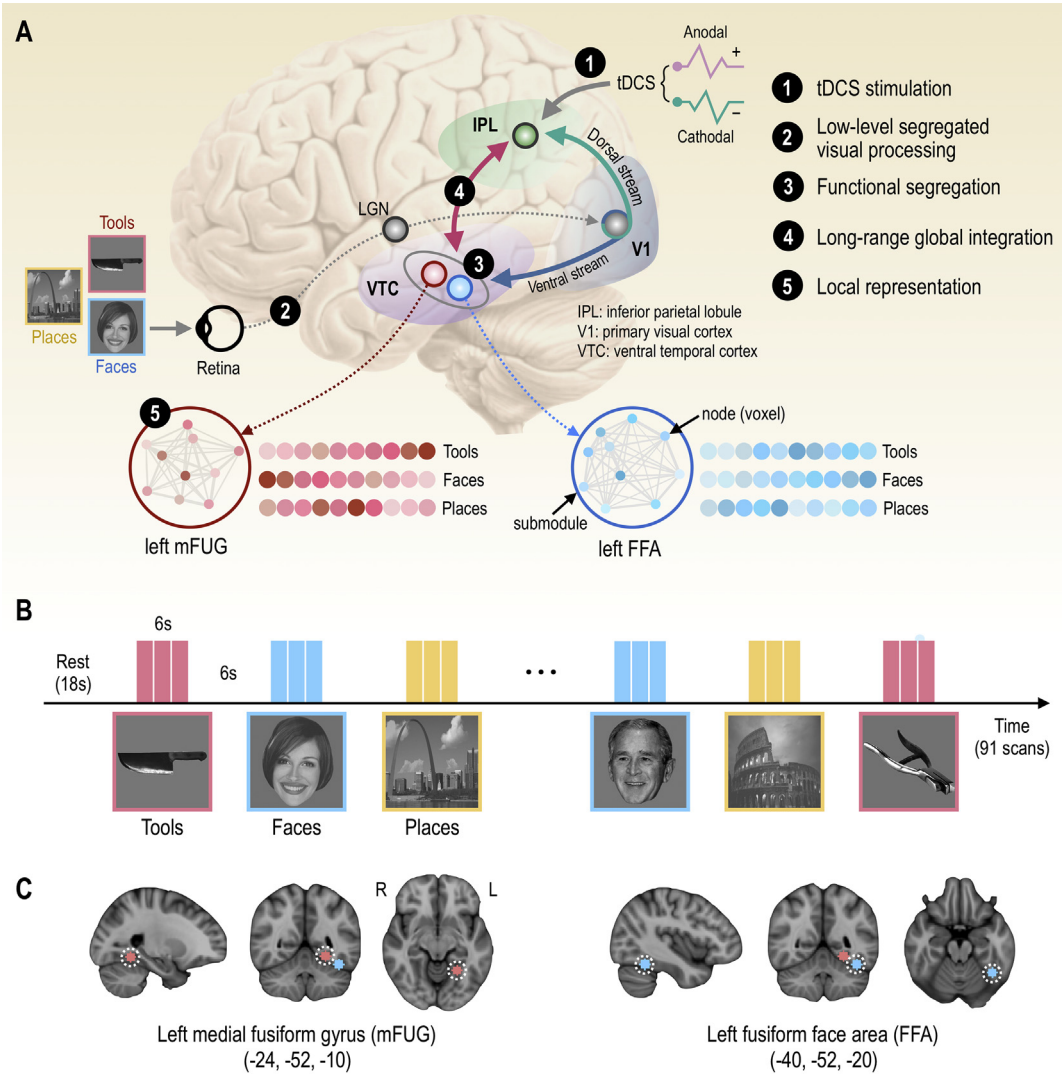

Fig. 1 – Experimental procedures and stimuli processing. (A) Schematic of stimulus processing in the context of the experimental procedures used in tDCS sessions 2 and 3. Participants viewed images of tools, faces, and places immediately after stimulation of left IPL with anodal or cathodal tDCS (1). Stimuli are processed in a feedforward fashion (2) leading to neural activity within segregated regions of ventral temporal cortex (3). Through long-range connectivity (4) category-specific information is integrated within a functionally-specified neural network and local representations are modulated and tuned in a category-specific manner (5); (B) an example of the experimental design used, in which category-specific blocks were interspaced with fixation-only blocks; and (C) the ventral temporal cortical regions of interest used in the subsequent analysis. These regions were defined around peak coordinates obtained in the literature.

1. Materials and methods

1.1. *Participants*

For the current study, we reanalyzed data from ten healthy subjects (5 males and 5 females, ages from 18 to 33 years, mean = 23.1, SD = 4.3) that participated in a previously published study (Almeida et al., 2017). This sample size is in line with some previous published papers (e.g., Chen et al., 2016). No participant was excluded from the experiment. We mention all manipulations, and all measures in the study. All subjects were right-handed with normal or corrected-to-normal vision, and had no history of neurological and psychiatric disorders. Our participants went through the typical questionnaires regarding MRI and tDCS safety. Our study was approved by the ethical committee of the Faculty of Psychology and Educational Sciences, University of Coimbra, and written informed consent was obtained from all subjects.

1.2. *Experiment*

All participants completed three fMRI sessions (plus another unrelated sessions that was not analyzed herein) each separated by at least a week: two with (anodal and cathodal sessions) and one without (control session) tDCS stimulation immediately prior to the fMRI experiment. The control session

was always the first session. The order of the remaining sessions was counterbalanced across participants. No part of the study procedures and analysis was pre-registered prior to the research being conducted.

1.2.1. *Transcranial direct current stimulation (tDCS)*

We used a tDCS stimulator (TCT Research Limited, Hong Kong, China) with 24.75 cm^2 sponge electrodes soaked in saline solution (.9%). The intensity of the current was set to 2 mA, and was delivered for 20 min. The target area for tDCS stimulation was the left IPL: in the anodal tDCS condition, the anode electrode was placed above the left IPL and the cathode electrode was placed on the participant's contralateral deltoid muscle, whereas in the cathodal tDCS condition, the electrodes were reversed. In the control session, no electrodes were placed as no electrical stimulation was applied. During stimulation, participants were told to rest, and were given no task. We used two strategies to locate left IPL. In 4 of the participants we defined left IPL individually in the participant's native space by using functional data from control sessions and contrasting responses for tool stimuli with responses for animal stimuli. We then used neuronavigation (Brainsight, Rogue Research) to set the stimulation site. In the remaining 6 individuals we made use of the 10/20 EEG system to define left IPL, and chose the location of the P3 electrode as our target area (Herwig, Satrapi, & Schonfeldt-Lecuona, 2003). These strategies are the most used strategies to locate the stimulation site in the literature.

The tDCS room was immediately adjacent to the MRI bore, allowing for a fast transfer to the MRI environment right after tDCS stimulation.

1.2.2. *fMRI object perception task*

Participants were presented with intact and scrambled gray-scaled images of tools, places, faces, animals, and were ask to pay attention and focus on the center of the screen. We obtained 91 volumes per run, with each run comprising 8 intact stimulus blocks (2 per category), 4 phase-scrambled stimulus blocks (1 per category). Stimulus blocks were separated by 6 s of fixation, and run started with 18 s of fixation and ended with 20 s of fixation. There were three volumes collected for each stimulus block. Each participant completed 5 experimental runs per session. Across runs different exemplars were used for the face, animal, tool and place stimuli to reduce repetition priming effects across runs. The stimuli were 400 × 400 pixels in size (~10° of visual angle) and presented on a gray background using an Avotec projector (Stuart, FL, USA) under 60 Hz refresh rate. This is a reanalysis of Almeida and Colleagues (Almeida et al., 2017), and as such, not all conditions from that study were conditions of interest in the current study. In particular, we focused only on the categories of tools, faces and places as a way of testing distal effects of tDCS. Study materials (and presentation code) can be obtained at https://doi.org/10.6084/m9.figshare.7631603.v2.

1.3. *Analysis*

1.3.1. *Data acquisition and image processing*

Whole-brain fMRI data were acquired with a Siemens Tim Trio 3-T MRI scanner (Siemens Healthineers, Erlangen, Germany) with a 12-channel head coil at the Portuguese Brain Imaging Network. High-resolution structural T1-weighted data were obtained using a MPRAGE (magnetization prepared rapid gradient echo) sequence with the following parameters: a 256 × 256 acquisition matrix, a 256 mm field-of-view, a voxel size of 1.0 × 1.0 × 1.0 mm^3, a repetition time (TR) of 2530 msec, and an echo time (TE) of 3.29 msec. fMRI data were acquired axially using T2*-weighted single-shot echo-planar imaging (EPI) sequence using the following parameters: a 64 × 64 acquisition matrix, a 256 mm field-of-view, 30 (interleaved) slices, a voxel size of 4.0 × 4.0 × 4.0 mm^3, a TR of 2000 msec, a TE of 30 msec, 90° flip angle, and no slice gap. Preprocessing of fMRI data was conducted using statistical parametric mapping (SPM12, http://www.fil.ion.ucl.ac.uk/spm/; Friston et al., 1995) . All functional data underwent standard preprocessing steps, including slice scan time correction, correction for head motion by realigning all consecutive volumes to the first image of the session, and co-registration of T1-weighted images to the first functional volume using the linear registration algorithm. Co-registered T1-images were used to spatially normalize functional data into MNI space using nonlinear transformation in SPM12. Functional data were interpolated to 2.0 × 2.0 × 2.0 mm^3 voxels. No spatial smoothing was conducted to avoid spill-over effects between voxels (Todd, Nystrom, & Cohen, 2013) and to avoid inflation of local connectivity (van den Heuvel, Stam, Boersma, & Hulshoff Pol, 2008). The conditions of our ethical approval do not permit anonymized study to be publicly archived. To obtain access to the data, authors should contact the corresponding author. Requests for data are assessed and approved by the ethical committee of the Faculty of Psychology and Educational Sciences, University of Coimbra.

1.3.2. *Regions of interest*

We defined 2 regions of interest within left ventral temporal cortex: a tool-preferring area, and a face-preferring area. The tool-preferring left mFUG was defined using the coordinates reported in Mahon and colleagues (Mahon et al. 2007); the face-preferring left FFA was defined using coordinates obtained using automated meta-analyses (http://neurosynth.org; Yarkoni, Poldrack, Nichols, Van Essen, & Wager, 2011) surveying 704 published studies on face processing. For each area, we created a 6 mm-radius sphere centered at the particular coordinates. All regions were composed of 123 functional voxels.

1.3.3. *Representational similarity analysis*

As a preprocessing step for representational similarity analysis, the fMRI data were linearly detrended at each experimental run to remove low frequency drifts of the fMRI time series and biases between runs. The detrended data were normalized by subtracting the mean and dividing by the standard deviation to reduce signal differences between runs. After linear detrending and normalization, the volumes within the blocks for tools and faces were resampled taking into consideration the hemodynamic delay in fMRI (peak at around 6 sec after stimulus onset = 3 volumes; repetition time [TR = 2 sec]). To avoid temporal overlapping of hemodynamic responses from other category blocks, only the second and third volumes were used in the resampling. Within each

region of interest, we extracted signal intensities, from the resampled dataset, per each of the 123 voxels for each of the resampled volumes. Overall, per category and per participant we extracted 20 separate neural patterns: 2 volumes per block, 2 blocks per run and 5 runs for each session. Thus we extracted a total of 60 neural patterns.

For representational similarity analysis, we calculated dissimilarity between these neural patterns in a pairwise fashion using correlation distance (i.e., 1 − Pearson's *r*). These distance values were organized in dissimilarity matrices (Representational Dissimilarity Matrices − RDMs) for each region and tDCS condition (anodal and cathodal) separately. When correlation distance increases, dissimilarity increases (low similarity), whereas when correlation distance decreases, dissimilarity decreases (high similarity). To facilitate the understanding of similarity between the patterns we calculated "Pattern similarity" defined as 2-dissimilarity; this measure ranges from 0 to 2, with 0 being no similarity and 2 being complete similarity.

To analyze the data, and as our main analysis, we first employed a 2 (Region: left mFUG *vs* left FFA) X 2 (Category: Tools *vs* Faces) X 2 (tDCS polarity: Anodal *vs* Cathodal) repeated measures ANOVA over tool and face-related pattern similarity, and inspected the triple order interaction. Depending on this triple order interaction, we then proceeded with testing for the simple effects using paired *t*-tests to compare pattern similarity between anodal and cathodal tDCS sessions for each category at the two regions of interest. As a control analysis, and in order to test for category-specificity, we performed the same analysis but substituted tool neural patterns by place neural patterns. That is, we employed a 2 (Region: left mFUG *vs* left FFA) X 2 (Category: Places *vs* Faces) X 2 (tDCS polarity: Anodal *vs* Cathodal) repeated measures ANOVA, and inspected the triple order interaction. Once again, depending on this triple order interaction, we tested for the simple effects.

1.3.4. *Pattern discriminability analysis*

Pattern discrimination analysis was carried out over the neural patterns that were described above (from the control, anodal and cathodal sessions). Voxel intensities in each neural pattern were used as features in the classification analysis. We used a binary linear classifier based on support vector machine (SVM) algorithms (e.g., Boser, Guyon, & Vapnik, 1992) to discriminate between tools and faces and separately between places and faces. We used data from the first (no-tDCS) fMRI session as the training data set (40 patterns in total, 20 per category) and the fMRI data following anodal and cathodal tDCS as the testing data sets (40 patterns in total). SVM classification was conducted using Spider for MATLAB (http://people.kyb.tuebingen.mpg.de/spider/). We trained a linear SVM classifier on the classification of tools versus faces or on the classification of places versus faces using a hyperparameter C = 1 (Andersson, Pluim, Viergever, & Ramsey, 2013; Sitaram et al., 2011). After SVM training, the classifier was used to classify new samples from the anodal or the cathodal tDCS sessions. Mean classification accuracy was calculated by averaging across the 40 classification decisions made by each classifier. Statistical comparisons were performed as above. We run two 2 (Region: left mFUG *vs* left FFA) X 2 (tDCS polarity: Anodal *vs* Cathodal) repeated measures ANOVA, one for the classification between tools and faces (our main analysis), and one for the control classification between places and faces (our control analysis), and inspected the interaction term. Depending on there being an interaction, we then proceeded with testing for the simple effects by using paired-sample t-tests over mean classification accuracy were carried out between the anodal and cathodal testing data.

2. Results

2.1. *Distal distortions in representational content*

Neural responses to tools and faces (see Fig. 1B; see Methods) were measured using whole brain fMRI in three different sessions in human participants (N = 10). In the first session, all participants completed the fMRI experiment with no neuromodulation prior to fMRI scanning. In the remaining two sessions for each participant, transcranial direct current stimulation was applied prior to fMRI scanning to modulate processing in the left IPL. We then measured neural responses in the left mFUG and the left FFA (see Fig. 1C) to images of tools, faces and places immediately after tDCS. In one tDCS session, anodal tDCS was administered to left IPL, and in the other session, cathodal tDCS was administered to left IPL (order counterbalanced across subjects).

Because we are interested in how content is represented, we focused on a multivariate analysis of our data. Specifically, we first visualized the 'distortions' in representational content in ventral temporal cortex using representational similarity analysis (Kriegeskorte, Mur, & Bandettini, 2008). If ventral temporal tool representations are distorted by tDCS to left IPL, then this should be visible as a change in the similarity between tool-selective neural patterns in the cathodal versus anodal tDCS conditions. We computed pairwise similarity between the neural patterns elicited by stimuli from tools, places and faces in the left mFUG, and left FFA (see Fig. 2A). Each cell within the dissimilarity matrices presented in Fig. 2A represents the distance (computed as 1-Pearson's r) between the neural patterns elicited by our stimuli across the voxels in our ventral temporal cortical regions for the anodal and cathodal sessions. These dissimilarity matrices are demonstrative of the categorical preferences across the two regions. Neural patterns elicited by the presentation of tool stimuli seemed overall more similar to one another in the left mFUG than in the left FFA, in a similar fashion to what is observed for the category of places, whereas similarity between the neural patterns elicited by face stimuli were stronger in the left FFA.

In order to statistically test for tDCS-induced distortions in the dissimilarity matrices we compared pattern similarity between anodal tDCS to left IPL and cathodal tDCS to left IPL for each category and region (Fig. 2B). We first focused on our main categories of interest – i.e., faces and tools. We observed an interaction between the region from which we collected the data (i.e., left mFUG and left FFA), the category of the stimuli (faces *vs* tools), and tDCS polarity ($F(1,9) = 4.92$, $p = .05$, $\eta^2 = .35$). Specifically, there was an increase in pattern similarity for tool items in the left mFUG after anodal tDCS (average similarity = 1.24, Standard Error of the Mean

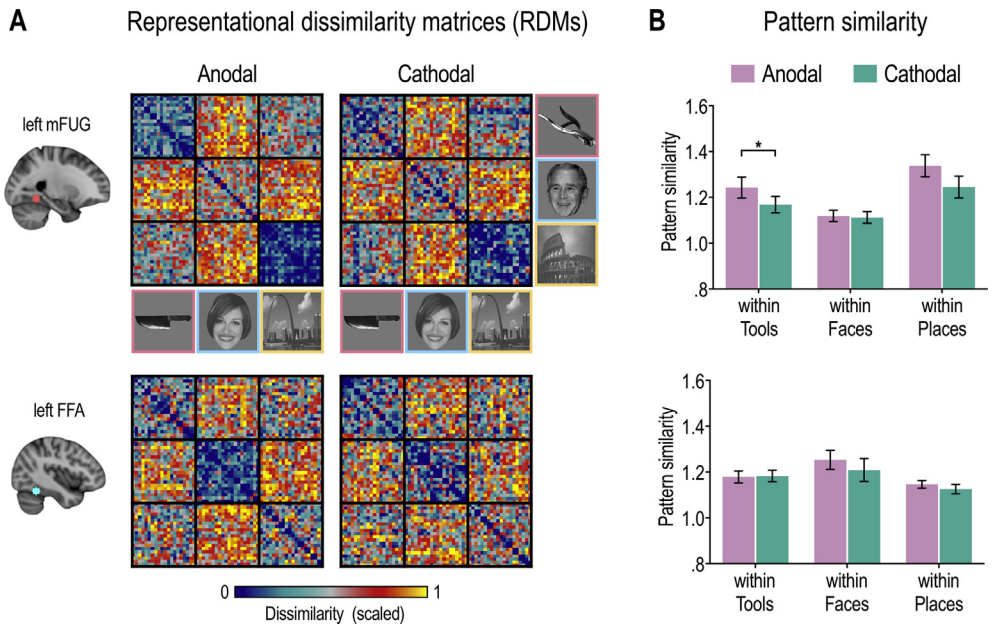

Fig. 2 – Distortions of object representational space in ventral temporal cortex following tDCS to left IPL. (A) Representational dissimilarity matrices for each tDCS condition on data from each ventral temporal region. Color codes for how dissimilar the voxels-wise patterns are (blue – no dissimilarity – to red – maximum dissimilarity) as measured using 1 – Pearson's r for the pairwise correlation. These dissimilarity matrices are demonstrative of the categorical preferences across the two regions; and (B) within-category pattern similarity (measured as 2 – dissimilarity) for each tDCS condition, category and ventral temporal region. Pattern similarity for tool items in the left mFUG is significantly lower in the cathodal than in the anodal tDCS condition. *$p < .05$.

(SEM) = .05) compared to cathodal tDCS to left IPL (average similarity = 1.17, SEM = .04; $t(9) = 2.83$; $p = .02$; Cohen's d for repeated measures = .89). Similar comparisons in left FFA did not result in differences between anodal and cathodal sessions ($t < 1$; Cohen's d for repeated measures = –.03). Pattern similarity for face stimuli was not affected by the polarity of tDCS to left IPL (statistics for comparisons of pattern similarity for faces in left mFUG and in left FFA were $t < 1$; Cohen's d for repeated measures = .14, and $t(9) = 1.48$; $p = .17$; Cohen's d for repeated measures = .47 respectively). Thus, tool similarity is more dispersed in the cathodal compared to the anodal tDCS stimulation condition (suggesting more dissimilar tool representations in the cathodal condition) when information is extracted from the left mFUG, an effect that is not visible for tools in the left FFA, nor for faces in any of the ROIs. As a control comparison we focused on the category of places and compared it again with the category of faces (Fig. 2B). In this analysis, the triple order interaction did not reach significance ($F(1,9) = 1.92$, $p = .20$, $\eta^2 = .18$). As such, the simple effects were not inspected.

2.2. *Distal effects of on pattern discriminability*

Multivoxel classification (e.g., Haxby et al., 2001; Norman, Polyn, Detre, & Haxby, 2006) was then employed to further assess how category-specific representations within regions of ventral temporal cortex were altered by tDCS applied to the left IPL. For each participant and for each session, voxel-wise patterns of object-selective responses (i.e., tools, faces, and places) were extracted for the 2 areas of interest within ventral temporal cortex. To maintain independence of voxel definition and voxel test, regions of interest were defined using peak coordinates from prior studies and meta-analytic procedures, as described in the methods. Voxel patterns from the first (no-tDCS control session) session were used to train SVM classifiers (e.g., Cortes & Vapnik, 1995). Those trained classifiers were tested on the category preferences elicited after anodal and cathodal tDCS sessions, and classification accuracy was compared between the two tDCS sessions. In our main analysis, the SVM classifier for each ventral temporal region was trained and tested to discriminate tool stimuli from face stimuli. In our control analysis, the SVM classifier for each ventral temporal region was trained and tested to discriminate place stimuli from face stimuli. This way, we could test whether the ability to represent category-specific information in each ventral temporal area was modulated by the polarity of tDCS over left IPL, and whether this modulation was specific to tools, and not more general to all information processed within a node. If the effects of stimulating the tool-preferring left IPL are specific to the tool network, then only the classifier trained on data from the left mFUG should be affected, and not the classifier trained on data from the left FFA. Moreover, if the effects are specific to tool stimuli, then there should be an effect of tDCS for the classification between tool stimuli and face stimuli, but no effect of tDCS for the classification between place stimuli and face stimuli.

The principal finding was that category discriminability in ventral temporal cortex was affected by anodal tDCS versus cathodal tDCS. As can be seen in Fig. 3A, the effect of tDCS over left IPL on category discriminability in ventral temporal cortex was specific for the left mFUG and not for the left FFA.

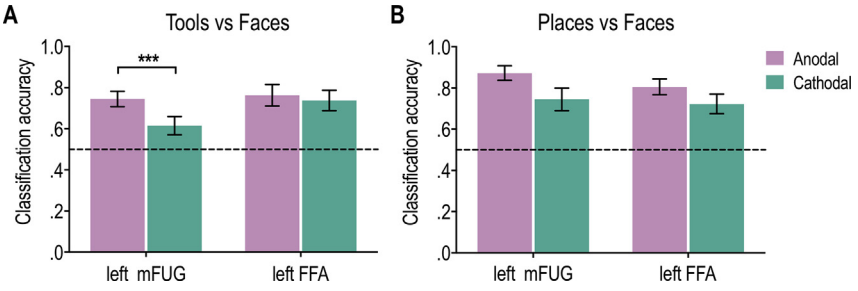

Fig. 3 – Modulation of category discriminability in ventral temporal cortex by tDCS to left IPL. Classification accuracy in each ventral temporal area, when tested with anodal or cathodal object-selective patterns of activation: (A) for the classification between tool stimuli and faces stimuli; and (B) for the classification between place stimuli and faces stimuli. Data shows that tDCS over left IPL disrupted tool discriminability in the left mFUG but not in the left FFA. $^{***}p < .001$.

Specifically, in our main analysis (i.e., the classification between tools and faces) we obtained an (marginally significant) interaction between the region of provenance of the data for classification and the polarity of the tDCS (F (1,9) = 4.47, $p = .06$, $\eta^2 = .33$). Simple effects showed that in the left mFUG, classification accuracy for discriminating tools versus faces after cathodal tDCS to left IPL (average accuracy = 61.5%; SEM = 4.4%) was significantly lower than after anodal tDCS to left IPL (average accuracy = 74.5%; SEM = 3.8%; t (9) = 5.83; $p = .0002$; Cohen's d for repeated measures = 1.84; Classifying tools versus faces in left FFA: $t < 1$; Cohen's d for repeated measures = .16). Importantly, in our control analysis we focused on the effects of tDCS to IPL on the classification between place and face stimuli. As in the Representational Similarity Analysis (RSA) analysis, the interaction for the control analysis did not reach significance (F (1,9) = 1.29, $p = .26$, $\eta^2 = .13$; Fig. 3B). As such, the simple effects were not inspected. These data indicate that perturbing processing within a remote tool-preferring region affects representations of tools in ventral temporal cortex, and demonstrates that content-defined neural networks can drive (online) neural responses in ventral temporal cortex.

Collectively, these findings show that perturbation of the left IPL affects information integration and representational content in ventral temporal cortex in a regionally and categorically-specific manner: voxels within the left mFUG exhibited tDCS-induced changes in the representational content for tool stimuli (and no changes in representational content for face or place stimuli), and these effects on representational content and pattern discriminability are specific to the left mFUG.

3. Discussion

Here we report causal evidence showing that neural representations in ventral temporal cortex can be driven by interactions with anatomically remote regions. Our data indicates that disrupting processing within a distal but connected region impacts local representations and pattern discriminability. We suggest that these local representations depend on information integration within a functionally-specified neural network, with large-scale connectivity tuning and modulating representations in the individual modules of the network. Importantly, this tuning seems to be network-specific and domain-specific, as voxels within a region may show or fail to show effects of altered neural dynamics according to their network membership and categorical preference, and as this tuning does not seem to spread unspecifically to neighboring areas.

Converging with this view are insights from the neurobiological phenomenon of diaschisis, whereby focal brain lesions affect neural processing in anatomically remote and physiologically intact regions (Carrera & Tononi, 2014; Garcea et al., 2018; Price, Warburton, Moore, Frackowiak, & Friston, 2001). Moreover, these data may provide a neural substrate for top-down attentional modulation effects (e.g., Reynolds & Chelazzi, 2004; Zhang & Kay, 2018) on occipital and temporal cortex, whereby responses are enhanced in tandem with attentional deployment and task demands. Finally, our proposal is line with the view that functional integration is achieved through large-scale connections between distributed cortical regions (Park & Friston, 2013; Varela, Lachaux, Rodriguez, & Martinerie, 2001), with one possible implementation of such networks being the emergence of connectivity-constrained neural assemblies that are dedicated to particular computational goals, and are supported by reciprocal interactivity and cell-firing synchronization (Chen et al., 2016; Mahon, 2015; Op de Beeck et al., 2008; Saygin et al., 2016; Varela et al., 2001).

In fact, there is a growing number of fMRI studies that have demonstrated functional interactions among distributed brain regions involved in visual processing of tools (e.g., Almeida et al., 2013; Chen et al., 2016; Hutchison et al., 2014), and faces (Hutchison et al., 2014; Pitcher, Duchaine, & Walsh, 2014; Pitcher, Japee, Rauth, & Ungerleider, 2017), suggesting that global integration of information from the different modules of a network should occur via long-range connectivity between these modules. This brings forth a potential mechanistic explanation for the disruption of information integration and representation observed at the left mFUG, whereby deficient transmission of information between modules of a network will disturb global integration of network-preferred information across the modules of the network.

In order to explore the potential importance of connectivity in driving our effects, and also as a way to determine whether the distal effects of tDCS observed over the representations within the left mFUG were traceable back to the left IPL, we performed a set of supplementary analysis on our

data. Specifically, we focused on the functional connectivity patterns of the left mFUG to the whole brain after cathodal and anodal tDCS, and on the effective connectivity between the left mFUG and the left IPL (see supplementary materials for detailed information on the methods used). Because the left IPL was the target area of tDCS, we predicted that functional connectivity between that area and the distally affected area (i.e., the left mFUG) should be differentially affected by the two tDCS conditions. Our whole brain functional connectivity results using the left mFUG as seed region showed that the left mFUG presents significantly increased functional connectivity with the left Supramarginal gyrus (SMG; a major region of the left IPL), and the left supplementary motor area (SMA) after anodal tDCS compared to cathodal tDCS (see supplementary materials for a detailed description of the results of this analysis; see Fig. S1).

Importantly, this decrement in information traversing from the left IPL and the left mFUG seems to be specific for tool information. We performed Psycho-physiological interaction (PPI) analysis (Friston et al., 1995) between the left IPL (and particularly left SMG) and the left mFUG, and show that the connectivity between these areas is influenced by the polarity of tDCS only when participants are processing tool stimuli, but not when they were processing other (e.g., place) stimuli (see supplementary materials for a detailed description of the results of this analysis; see Fig. S1). That is, the decrement in information exchange between the left IPL and the left mFUG is specific for when participants are processing tool stimuli and not stimuli from other categories, suggesting that the effect visible at the left mFUG can be traced back to the left IPL despite the fact that tDCS is not a very focal technique, and that global information integration within a network is highly specific to the type of information that the network is specialized in. Our supplementary data on functional and effectivity connectivity are then in line with this possible deficient transmission of information hypothesis – functional and effective connectivity are causally changed by tDCS stimulation disturbing global integration of information that is specific to the submodules of the tool network, and to tool-related information.

One aspect that may not be fully resolved with these data is whether the distal effects obtained herein are dictated by long-distance but direct effects of tDCS onto the left mFUG, or whether these effects are rather due to local disruptions at the site of stimulation that transpire down in terms of the passage of information from the left IPL to the left mFUG. Importantly, we have previously shown over this same data that neural responses for tools within tDCS-stimulated left IPL are dependent on the polarity of stimulation (Almeida et al., 2017). This strongly suggests that distorted representations in IPL are causally modulating representational content in the left mFUG.

One outstanding topic in the field of tDCS that warrants some discussion is whether cathodal and anodal stimulation lead, necessarily, to cortical inhibition and excitation respectively. Batsikadze and collaborators (Batsikadze et al., 2013) showed that this may be dependent on the stimulation parameters used. Specifically, they showed that unlike the use of 1 mA stimulation, the use of 2 mA – now widespread in cognitive and clinical applications – over motor cortex leads to cortical excitability irrespective of whether the simulation was anodal or cathodal. This is certainly important for our study as we have used a stimulation intensity of 2 mA. However, we have shown previously on these same data and participants that tool-specific responses at the site of our stimulation (IPL) are modulated by tDCS stimulation in a polarity-specific way – i.e., the magnitude of tool-specific responses in left IPL increased under anodal stimulation and decreased under cathodal stimulation (Almeida et al., 2017). It is possible that the difference between the results of Almeida et al. (2017) and those of Batsikadze et al. (2013) are due to the area of stimulation (left IPL versus motor cortex), and potential differences in the physiological responses of these regions. Future studies should focus on whether difference regions are differentially affected by different tDCS stimulation parameters. Another aspect that is important in the tDCS literature, and that the methods used here and data obtained cannot adjudicate is whether neuronavigation systems should be used in lieu of the traditional EEG 10–20 system to locate target areas. In this paper we used both neuronavigation and the EEG system to locate left IPL, but we did so in different participants. This is a limitation of our study, as we do not have enough statistical power to address this question.

To sum up, here we show that tDCS stimulation in a distal but category- and network-related module causally affects categorical representations and pattern discriminability locally.

CRediT authorship contribution statement

Dongha Lee: Formal analysis, Data curation, Writing - original draft. **Bradford Z. Mahon:** Writing - review & editing. **Jorge Almeida:** Conceptualization, Funding acquisition, Supervision, Formal analysis, Data curation, Writing - original draft, Writing - review & editing.

Open practices

The study in this article earned the Open Materials badge for transparent practices. Materials and data for the study are available at https://doi.org/10.6084/m9.figshare.7631603.v2.

Acknowledgments

This work was supported by a Foundation for Science and Technology of Portugal and Programa COMPETE grant (PTDC/PSI-GER/30745/2017), and by an European Research Council Starting Grant ("ContentMAP" - 802553) to JA. DL is supported by a Foundation for Science and Technology of Portugal and Programa COMPETE grant (PTDC/MHC-PCN/6805/2014). Preparation of this MS was supported, in part, by NSF grant BCS-1349042 and NIH Grants R01NS089069 and R01EY028535 to BZM. We thank Daniela Valério, Ana Rita Martins, Lénia Amaral, Ana Ganho-Ávila, Joana Nogueira, Andreia Freixo, and Stephanie Kristensen for their help in data collection.

Supplementary data

Supplementary data to this article can be found online at https://doi.org/10.1016/j.cortex.2019.02.018.

REFERENCES

Almeida, J., Fintzi, A. R., & Mahon, B. Z. (2013). Tool manipulation knowledge is retrieved by way of the ventral visual object processing pathway. *Cortex; A Journal Devoted to the Study of the Nervous System and Behavior, 49*(9), 2334–2344. https://doi.org/10.1016/j.cortex.2013.05.004.

Almeida, J., Martins, A. R., Bergstrom, F., Amaral, L., Freixo, A., Ganho-Avila, et al. (2017). Polarity-specific transcranial direct current stimulation effects on object-selective neural responses in the inferior parietal lobe. *Cortex; A Journal Devoted to the Study of the Nervous System and Behavior, 94*, 176–181. https://doi.org/10.1016/j.cortex.2017.07.001.

Andersson, P., Pluim, J. P., Viergever, M. A., & Ramsey, N. F. (2013). Navigation of a telepresence robot via covert visuospatial attention and real-time fMRI. *Brain Topography, 26*(1), 177–185. https://doi.org/10.1007/s10548-012-0252-z.

Batsikadze, G., Moliadze, V., Paulus, W., Kuo, M. F., & Nitsche, M. A. (2013). Partially non-linear stimulation intensity-dependent effects of direct current stimulation on motor cortex excitability in humans. *J Physiol, 591*(7), 1987–2000.

Boser, B. E., Guyon, I., & Vapnik, V. (1992). A training algorithm for optimal margin classifiers. In *Proceedings of the Fifth Annual Workshop on Computational Learning Theory* (pp. 144–152).

Carrera, E., & Tononi, G. (2014). Diaschisis: Past, present, future. *Brain, 137*(Pt 9), 2408–2422. https://doi.org/10.1093/brain/awu101.

Chao, L. L., Haxby, J. V., & Martin, A. (1999). Attribute-based neural substrates in temporal cortex for perceiving and knowing about objects. *Nature Neuroscience, 2*(10), 913–919. https://doi.org/10.1038/13217.

Chao, L. L., & Martin, A. (2000). Representation of manipulable man-made objects in the dorsal stream. *NeuroImage, 12*(4), 478–484. https://doi.org/10.1006/nimg.2000.0635.

Chen, Q., Garcea, F. E., Almeida, J., & Mahon, B. Z. (2017). Connectivity-based constraints on category-specificity in the ventral object processing pathway. *Neuropsychologia, 105*, 184–196. https://doi.org/10.1016/j.neuropsychologia.2016.11.014.

Chen, Q., Garcea, F. E., & Mahon, B. Z. (2016). The representation of object-directed action and function knowledge in the human brain. *Cerebral Cortex, 26*(4), 1609–1618. https://doi.org/10.1093/cercor/bhu328.

Cortes, C., & Vapnik, V. (1995). Support-vector network. *Machine Learning, 20*, 273–297.

Deco, G., Jirsa, V. K., & McIntosh, A. R. (2011). Emerging concepts for the dynamical organization of resting-state activity in the brain. *Nature Reviews. Neuroscience, 12*(1), 43–56. https://doi.org/10.1038/nrn2961.

Deco, G., Tononi, G., Boly, M., & Kringelbach, M. L. (2015). Rethinking segregation and integration: Contributions of whole-brain modelling. *Nature Reviews. Neuroscience, 16*(7), 430–439. https://doi.org/10.1038/nrn3963.

DiCarlo, J. J., Zoccolan, D., & Rust, N. C. (2012). How does the brain solve visual object recognition? *Neuron, 73*(3), 415–434. https://doi.org/10.1016/j.neuron.2012.01.010.

Downing, P. E., Jiang, Y., Shuman, M., & Kanwisher, N. (2001). A cortical area selective for visual processing of the human body. *Science, 28*(5539), 2470–2473.

Epstein, R., & Kanwisher, N. (1998). A cortical representation of the local visual environment. *Nature, 392*(6676), 598–601. https://doi.org/10.1038/33402.

Fertonani, A., & Miniussi, C. (2016). Transcranial electrical stimulation: What we know and do not know about mechanisms. *The Neuroscientist*. https://doi.org/10.1177/1073858416631966.

Fregni, F., Boggio, P. S., Mansur, C. G., Wagner, T., Ferreira, M. J., Lima, C., et al. (2005). Transcranial direct current stimulation of the unaffected hemisphere in stroke patients. *NeuroReport, 16*(14), 1551–1555.

Friston, K., Holmes, A., Worsley, K., Poline, J., Frith, C., & Frackowiak, R. (1995). Statistical parametric maps in functional imaging: A general linear approach. *Human Brain Mapping, 2*, 189–210.

Garcea, F. E., Almeida, J., Sims, M. H., Nunno, A., Meyers, S. P., Li, Y. M., & Mahon, B. Z. (2018). Domain-specific diaschisis: Lesions to parietal action areas modulate neural responses to tools in the ventral stream. *Cerebral Cortex*. https://doi.org/10.1093/cercor/bhy183.

Garcea, F. E., Kristensen, S., Almeida, J., & Mahon, B. Z. (2016). Resilience to the contralateral visual field bias as a window into object representations. *Cortex; A Journal Devoted to the Study of the Nervous System and Behavior, 81*, 14–23. https://doi.org/10.1016/j.cortex.2016.04.006.

Garcea, F. E., & Mahon, B. Z. (2014). Parcellation of left parietal tool representations by functional connectivity. *Neuropsychologia, 60*, 131–143. https://doi.org/10.1016/j.neuropsychologia.2014.05.018.

Gauthier, I., Tarr, M. J., Anderson, A. W., Skudlarski, P., & Gore, J. C. (1999). Activation of the middle fusiform 'face area' increases with expertise in recognizing novel objects. *Nature Neuroscience, 2*(6), 568–573. https://doi.org/10.1038/9224.

Gill, J., Shah-Basak, P. P., & Hamilton, R. (2015). It's the thought that counts: Examining the task-dependent effects of transcranial direct current stimulation on executive function. *Brain Stimulation, 8*(2), 253–259.

Goodale, M. A., & Milner, A. D. (1992). Separate visual pathways for perception and action. [Review]. *Trends in Neurosciences, 15*(1), 20–25.

Grill-Spector, K., Kushnir, T., Edelman, S., Avidan, G., Itzchak, Y., & Malach, R. (1999). Differential processing of objects under various viewing conditions in the human lateral occipital complex. *Neuron, 24*(1), 187–203.

Grill-Spector, K., & Malach, R. (2004). The human visual cortex. *Annual Review of Neuroscience, 27*, 649–677.

Haxby, J. V., Gobbini, M. I., Furey, M. L., Ishai, A., Schouten, J. L., & Pietrini, P. (2001). Distributed and overlapping representations of faces and objects in ventral temporal cortex. *Science, 293*(5539), 2425–2430. https://doi.org/10.1126/science.1063736.

Herwig, U., Satrapi, P., & Schonfeldt-Lecuona, C. (2003). Using the international 10-20 EEG system for positioning of transcranial magnetic stimulation. *Brain Topography, 16*(2), 95–99.

Hutchison, R. M., Culham, J. C., Everling, S., Flanagan, J. R., & Gallivan, J. P. (2014). Distinct and distributed functional connectivity patterns across cortex reflect the domain-specific constraints of object, face, scene, body, and tool category-selective modules in the ventral visual pathway. *NeuroImage, 96*, 216–236. https://doi.org/10.1016/j.neuroimage.2014.03.068.

Hutchison, R. M., & Gallivan, J. P. (2016). Functional coupling between frontoparietal and occipitotemporal pathways during action and perception. *Cortex; A Journal Devoted to the Study of the Nervous System and Behavior, 98*, 8–27. https://doi.org/10.1016/j.cortex.2016.10.020.

James, T. W., Humphrey, G. K., Gati, J. S., Menon, R. S., & Goodale, M. A. (2002). Differential effects of viewpoint on

object-driven activation in dorsal and ventral streams. *Neuron, 35*(4), 793–801.
Kanwisher, N., McDermott, J., & Chun, M. M. (1997). The fusiform face area: A module in human extrastriate cortex specialized for face perception. *The Journal of Neuroscience, 17*(11), 4302–4311.
Kravitz, D. J., Peng, C. S., & Baker, C. I. (2011). Real-world scene representations in high-level visual cortex: It's the spaces more than the places. *The Journal of Neuroscience, 31*(20), 7322–7333. https://doi.org/10.1523/JNEUROSCI.4588-10.2011.
Kravitz, D. J., Saleem, K. S., Baker, C. I., Ungerleider, L. G., & Mishkin, M. (2013). The ventral visual pathway: An expanded neural framework for the processing of object quality. *Trends in Cognitive Sciences, 17*(1), 26–49. https://doi.org/10.1016/j.tics.2012.10.011.
Kriegeskorte, N., Mur, M., & Bandettini, P. (2008). Representational similarity analysis – connecting the branches of systems neuroscience. *Frontiers in Systems Neuroscience, 2*, 4. https://doi.org/10.3389/neuro.06.004.2008.
Kristensen, S., Garcea, F. E., Mahon, B. Z., & Almeida, J. (2016). Temporal frequency tuning reveals interactions between the dorsal and ventral visual streams. *Journal of Cognitive Neuroscience, 28*(9), 1295–1302. https://doi.org/10.1162/jocn_a_00969.
López-Alonso, V., Cheeran, B., Río-Rodríguez, D., & Fernández-del-Olmo, M. (2014). Inter-individual variability in response to non-invasive brain stimulation paradigms. *Brain Stimulation, 7*(3), 372–380.
Mahon, B. Z. (2015). *Missed connections: A connectivity constrained account of the representation and organization of object concepts*.
Mahon, B. Z., Kumar, N., & Almeida, J. (2013). Spatial frequency tuning reveals interactions between the dorsal and ventral visual systems. *Journal of Cognitive Neuroscience, 25*(6), 862–871. https://doi.org/10.1162/jocn_a_00370.
Mahon, B. Z., Milleville, S. C., Negri, G. A., Rumiati, R. I., Caramazza, A., & Martin, A. (2007). Action-related properties shape object representations in the ventral stream. *Neuron, 55*(3), 507–520. https://doi.org/10.1016/j.neuron.2007.07.011.
Martins, A. R., Fregni, F., Simis, M., & Almeida, J. (2017). Neuromodulation as a cognitive enhancement strategy in healthy older adults: Promises and pitfalls. *Neuropsychology, Development, and Cognition. Section B, Aging, Neuropsychology and Cognition, 24*(2), 158–185. https://doi.org/10.1080/13825585.2016.1176986.
Noppeney, U., Price, C. J., Penny, W. D., & Friston, K. J. (2006). Two distinct neural mechanisms for category-selective responses. *Cerebral Cortex, 16*(3), 437–445. https://doi.org/10.1093/cercor/bhi123.
Norman, K. A., Polyn, S. M., Detre, G. J., & Haxby, J. V. (2006). Beyond mind-reading: Multi-voxel pattern analysis of fMRI data. *Trends in Cognitive Sciences, 10*(9), 424–430. https://doi.org/10.1016/j.tics.2006.07.005.
Op de Beeck, H. P., Haushofer, J., & Kanwisher, N. G. (2008). Interpreting fMRI data: Maps, modules and dimensions. *Nature Reviews. Neuroscience, 9*(2), 123–135. https://doi.org/10.1038/nrn2314.
Orban, G. A. (2008). Higher order visual processing in macaque extrastriate cortex. *Physiological Reviews, 88*(1), 59–89. https://doi.org/10.1152/physrev.00008.2007.
Park, H. J., & Friston, K. (2013). Structural and functional brain networks: From connections to cognition. *Science, 342*(6158), 1238411. https://doi.org/10.1126/science.1238411.
Pitcher, D., Duchaine, B., & Walsh, V. (2014). Combined TMS and FMRI reveal dissociable cortical pathways for dynamic and static face perception. *Current Biology, 24*(17), 2066–2070. https://doi.org/10.1016/j.cub.2014.07.060.
Pitcher, D., Japee, S., Rauth, L., & Ungerleider, L. G. (2017). The superior temporal sulcus is causally connected to the amygdala: A combined TBS-fMRI study. *The Journal of Neuroscience, 37*(5), 1156–1161. https://doi.org/10.1523/JNEUROSCI.0114-16.2016.
Price, C. J., & Devlin, J. T. (2011). The interactive account of ventral occipitotemporal contributions to reading. *Trends in Cognitive Sciences, 15*(6), 246–253. https://doi.org/10.1016/j.tics.2011.04.001.
Price, C. J., Warburton, E. A., Moore, C. J., Frackowiak, R. S., & Friston, K. J. (2001). Dynamic diaschisis: Anatomically remote and context-sensitive human brain lesions. *Journal of Cognitive Neuroscience, 13*(4), 419–429.
Quiroga, R. Q., Reddy, L., Kreiman, G., Koch, C., & Fried, I. (2005). Invariant visual representation by single neurons in the human brain. *Nature, 435*(7045), 1102–1107. https://doi.org/10.1038/nature03687.
Reynolds, J. H., & Chelazzi, L. (2004). Attentional modulation of visual processing. *Annual Review of Neuroscience, 27*, 611–647. https://doi.org/10.1146/annurev.neuro.26.041002.131039.
Rolls, E. T. (2000). Functions of the primate temporal lobe cortical visual areas in invariant visual object and face recognition. *Neuron, 27*(2), 205–218.
Rushworth, M. F., Behrens, T. E., & Johansen-Berg, H. (2006). Connection patterns distinguish 3 regions of human parietal cortex. *Cerebral Cortex, 16*(10), 1418–1430. https://doi.org/10.1093/cercor/bhj079.
Saygin, Z. M., Osher, D. E., Norton, E. S., Youssoufian, D. A., Beach, S. D., Feather, J., & Kanwisher, N. (2016). Connectivity precedes function in the development of the visual word form area. *Nature Neuroscience, 19*(9), 1250–1255. https://doi.org/10.1038/nn.4354.
Senço, N. M., Huang, Y., D'Urso, G., Parra, L. C., Bikson, M., Mantovani, A., et al. (2015). Transcranial direct current stimulation in obsessive-compulsive disorder: Emerging clinical evidence and considerations for optimal montage of electrodes. *Expert Review of Medical Devices, 12*(4), 381–391. https://doi.org/10.1586/17434440.2015.1037832.
Simmons, W. K., & Martin, A. (2012). Spontaneous resting-state BOLD fluctuations reveal persistent domain-specific neural networks. *Social Cognitive and Affective Neuroscience, 7*(4), 467–475. https://doi.org/10.1093/scan/nsr018.
Sitaram, R., Lee, S., Ruiz, S., Rana, M., Veit, R., & Birbaumer, N. (2011). Real-time support vector classification and feedback of multiple emotional brain states. *NeuroImage, 56*(2), 753–765. https://doi.org/10.1016/j.neuroimage.2010.08.007.
Stagg, C. J., & Nitsche, M. A. (2011). Physiological basis of transcranial direct current stimulation. *The Neuroscientist, 17*(1), 37–53. https://doi.org/10.1177/1073858410386614.
Stevens, W. D., Tessler, M. H., Peng, C. S., & Martin, A. (2015). Functional connectivity constrains the category-related organization of human ventral occipitotemporal cortex. *Human Brain Mapping, 36*(6), 2187–2206. https://doi.org/10.1002/hbm.22764.
Todd, M. T., Nystrom, L. E., & Cohen, J. D. (2013). Confounds in multivariate pattern analysis: Theory and rule representation case study. *NeuroImage, 77*, 157–165. https://doi.org/10.1016/j.neuroimage.2013.03.039.
van den Heuvel, M. P., Stam, C. J., Boersma, M., & Hulshoff Pol, H. E. (2008). Small-world and scale-free organization of voxel-based resting-state functional connectivity in the human brain. *NeuroImage, 43*(3), 528–539. https://doi.org/10.1016/j.neuroimage.2008.08.010.
Varela, F., Lachaux, J. P., Rodriguez, E., & Martinerie, J. (2001). The brainweb: Phase synchronization and large-scale integration. *Nature Reviews. Neuroscience, 2*(4), 229–239. https://doi.org/10.1038/35067550.
Vuilleumier, P., Henson, R. N., Driver, J., & Dolan, R. J. (2002). Multiple levels of visual object constancy revealed by event-

related fMRI of repetition priming. *Nature Neuroscience*, 5(5), 491–499. https://doi.org/10.1038/nn839.

Yarkoni, T., Poldrack, R. A., Nichols, T. E., Van Essen, D. C., & Wager, T. D. (2011). Large-scale automated synthesis of human functional neuroimaging data. *Nature Methods*, *8*(8), 665–670. https://doi.org/10.1038/nmeth.1635.

Zhang, R., & Kay, K. (2018). *Flexible top-down modulation in human ventral temporal cortex*. bioRxiv.